Electrical Impedance Spectroscopy Sensorised Needle for Prostate Cancer Localisation During MRI-Ultrasound-Fused Targeted Biopsy ⋆ ⋆⋆

Conor McDermott[1], Nicola Schieda[2], and Carlos Rossa[1]

[1] Carleton University, Ottawa ON K1S 5B6, Canada
[2] University of Ottawa, Ottawa ON K1N 6N5 Canada

Abstract. Prostate cancer (PCa) diagnosis has undergone a dramatic evolution in recent years. Men with clinical risk factors and important lesions observed via magnetic resonance imaging (MRI) typically undergo a targeted biopsy. In a typical prostate biopsy procedure, the operator uses ultrasound (US) imaging to place a biopsy needle in the lesion(s) identified pre-operation via MRI for sampling. However, there is no way to ascertain that the needle is correctly placed in the lesion before sampling. Thus, negative biopsy results occur and lead to uncertainty in treatment decisions.
This paper investigates the feasibility of using an instrumented needle probe that uses electrical impedance spectroscopy to identify the tissue at the needle tip in real-time based on the tissue's bioelectrical properties. A new probe is designed, constructed, and validated on a collected dataset of *ex-vivo* tissue samples. Several classification algorithms are then used and compared, with classifications accuracies over 90% in most cases. These preliminary results suggest that the use of sensorised biopsy needles for tissue identification could improve confidence in biopsy results, and reduce procedure time and number of biopsies performed.

Keywords: Electrical impedance spectroscopy · sensitivity analysis · experimental validation.

1 Introduction

Prostate cancer (PCa) is the most common malignancy and the third highest cause of cancer death in Canadian males [23]. Worldwide, it is estimated that out of 10.1 million cancer cases in males and 5.5 million cancer deaths in 2022 alone, prostate cancer makes up 7.3% of diagnoses and nearly 7% of deaths [6]. Despite its prevalence and effect on public health, little is known about PCa-specific risk factors [14]. Needle biopsies are the only way to confirm that cancerous exist inside the prostate [8]. The typical pathway for PCa biopsy is based on routine screening. If the screening indicates a lesion may be present, a prostate specific antigen (PSA) test will be conducted. If results indicate that a lesion may be present, a digital rectal examination will be performed, which will tend to be informative on the risk associated with the disease's development. If both the PSA and digital rectal examination are abnormal, it is advised to perform a needle biopsy in order to histologically examine tissue from the prostate [4, 18].

To obtain tissue to be sent for histological examination, the lesion must be accurately sampled. Historically, all sampling was done via non-targetted US guided biopsy, where the prostate is randomly sampled in a grid pattern. Recently, and most commonly, MRI-US targeted biopsy is performed alongside non-targetted US guided biopsy to improve detection. Targeted biopsy is a general term for a biopsy that uses image guidance to locate a lesion in the prostate, and attempts to position the needle inside the lesion before a

⋆ This research is supported by the Cancer Research Society and the Canadian Institutes of Health Research (grant #944486).
⋆⋆ Cette recherche est appuyée par la Société de recherche sur le cancer et les Instituts de recherche en santé du Canada (subvention no 944486).

sample is taken. MRI-TRUS targeted biopsy takes pre-operative MRI images and fuses them onto the US images in real-time using either cognitive, i.e., manual, or software registration techniques to aid the biopsy operator in locating the location of the lesion in the US images. An example is seen in Figure 1c where the location of the target previously identified in the MRI images is estimated in the US image in real-time. It is then sufficient to position the needle in the target via US imaging for sampling. Biopsies using MRI-US guidance may be more accurate than a biopsy acting on US alone, but the accuracy is highly dependent on lesion size, location, and the level of clinical suspicion from MRI images, i.e., the PI-RADS score [7].

Following a positive biopsy result, most patients undergo definitive therapy. A negative result, however, has uncertain implications. A negative result can be due to inaccurate localisation of the lesion, e.g., due to poor fusion of the MRI-detected lesion onto the US image, or from poor sampling i.e., the biopsy needle was not inserted into the target adequately. Interpretation of MRI may be incorrect due to operator error or the presence of other diseases that mimic cancer in MRI images [25]. A potential solution to overcome these limitations is to provide additional information to the biopsy operator in real-time, for example, the electrical or mechanical characteristics of the tissue at the biopsy needle tip, thereby indicating the location of the needle tip relative to landmarks visible in the MRI or US images. Ensuring that the needle tip is placed within the target before sampling could improve biopsy efficiency and accuracy and diagnostic yield, reduce procedure time, the number of samples taken and patient morbidity, and provide greater confidence in the event of a negative biopsy result [15].

It is known that the mechanical, optical, chemical, and electrical properties of malignant tissue differ from that of healthy tissue [1–3, 24, 12]. Electrical impedance spectroscopy (EIS) is a method of characterising the electrical impedance of a medium at various frequencies [20]. It works by injecting an electrical potential at various frequencies into the medium and measuring the current response, from which the medium's impedance is inferred. Therein, a spectrum representing the magnitude and phase response of the medium can be constructed. The measured spectrum of a tissue is typically characteristic of the tissue, or highly contrasted relative to other tissues, and can be used to discern one from another. However, there are a number of challenges related to integrating EIS sensors into surgical needles. First, the sensors must fit into the form factor of conventional biopsy needles, which generally have an outer diameter not exceeding 2 mm. This entails that the sensor must be long and slender, yet capable of maintaining rigidity to pierce tissue without deflecting. Second, the sensors must capture EIS spectra with high accuracy to discern different tissue types, i.e., the probe must be sensitive to small changes in electrical impedance. Third, data must be collected quickly and repeatably for the tool to be useful in real-time tissue characterisation.

Furthermore, there are a number of essential considerations when designing an EIS probe for biomedical applications including material selections, stimulation bandwidth, probe geometry, and electrode configuration. Material selection must ensure that the probe can be sterilised and bio-compatible, that is, when in contact with living tissues the probe does not produce adverse effects [26, 5]. The size of the probe and stray capacitance's can affect the probe's electrical sensitivity. A probe with high electrical sensitivity focuses the measurements into a smaller volume, ensuring that the tissue measured is in fact what is directly in front of the probe. In addition, an EIS probe must be compatible in form with equipment that is already in regular use. This limits many of the physical characteristics of a probe as most prostate biopsies are carried out using 16, 17, or 18 gauge needles.

Electrode configuration is also an important design consideration. The two most prevalent configurations are tetrapolar, and bipolar. Bipolar electrodes apply an AC voltage to the medium under test while the resultant current is measured in series simultaneously. With this configuration, the inferred complex impedance is subjected to local polarisations at the surface of both electrodes [9]. Conversely, a tetrapolar electrode configuration decouples the excitation and measurement electrodes so that the measurement is not influenced by polarisation, leading to more precise measurements [17, 19]. However, additional electrodes can be difficult to manufacture and implement into probes with small form factors.

Several different EIS-measuring needle probe designs have been proposed. An electrical bioimpedance measuring probe for *ex-vivo* prostate cancer detection is presented in [12]. The probe has a flat end and is

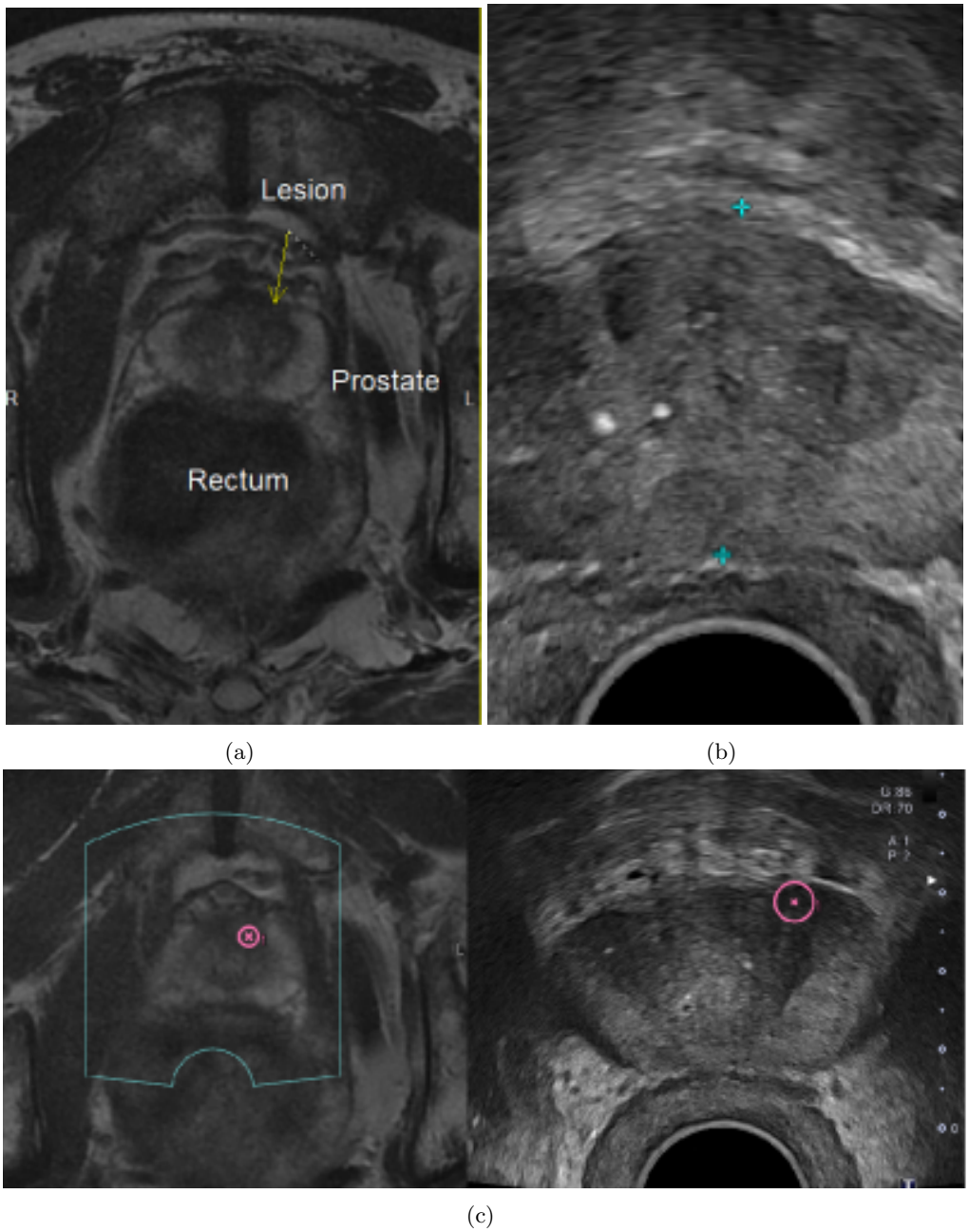

(a) (b)

(c)

Fig. 1: In a an MRI image of the prostate shows a potential lesion, which is not visible in the corresponding US images shown in b. MRI-US image registration shown in c is then performed to infer the position of the lesion in the US images given anatomical landmarks in both images.

3.5 mm in diameter in a coaxial, bipolar configuration. An EIS sensing biopsy needle made from a modified

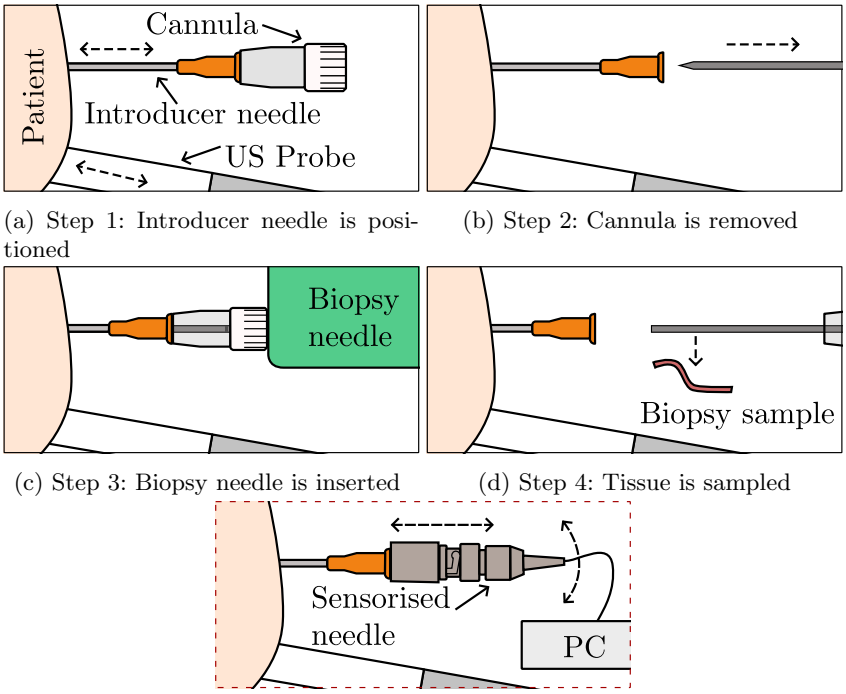

(a) Step 1: Introducer needle is positioned

(b) Step 2: Cannula is removed

(c) Step 3: Biopsy needle is inserted

(d) Step 4: Tissue is sampled

(e) Step 2.5: Between Steps 2 and 3, the sensorised needle is used to locate the target

Fig. 2: a shows Step 1, where the introducer needle and cutting cannula are inserted into the approximate area of the prostate. b is Step 2 where the cannula is removed, leaving the introducer needle in the intended area. c is Step 3, shows the biopsy needle inserted into the introducer needle to take samples. d shows Step 4, where the biopsy needle is removed and biopsy sample extracted. Thereafter, these 4 steps are repeated until operation completion. e shows Step 2.5, placed between steps 2 and 3, the proposed change to the procedure wherein the sensorised probe is placed into the introducer needle to locate the cancerous tissue.

18 GA stainless steel biopsy needle is presented in [22, 21, 13]. The probe was used to both measure the electrical impedance and extract biopsy cores, followed by the corresponding histological analysis [22].

Similarly, the Injeq needle from [10] is manufactured to match the dimensions of 18-gauge biopsy equipment and features an eccentric electrode geometry in a bipolar configuration. The eccentric electrode geometry gives the needle more highly localised sensitivity, ensuring that the measured electrical impedance is that of the tissue that is directly in front of the facet of its tip, but requires more complex manufacturing. Experimental work done in *in-vivo* porcine model validated the probes sensitivity [11].

Another design manufactures the EIS sensing circuit directly at the tip of a 22 GA needle [27]. The electrodes are manufactured in a bipolar interdigitated manner, as opposed to the more common coaxial configuration. The needle was used to discriminate cancerous renal tissue from healthy and shown experimentally to be able to characterise the maximum depth of endophytic tumours during partial nephrectomy to reduce surgical margins [28].

In [16], a design consisting of an 18-gauge bipolar stainless steel brachytherapy needle uses the needle shaft as the outer electrode and an electrically insulated copper core as the inner electrode. Polytetrafluoroethylene (PTFE) tubing chemically bonded with the inner electrode is used as the insulating material. The probe

was evaluated first through an equivalent circuit to verify its impedance, then through a series of *ex-vivo* and phantom tissue experiments. The probe can measure electrical impedance with sufficient sensitivity to be used with various classification algorithms.

This paper presents a new EIS instrumented biopsy needle and a large collected *ex-vivo* animal tissue dataset. Through the use of six down-stream machine learning models, preliminary validation is done to show the probe's ability to collect data in a repeatable manner and have it classified accurately. The down-stream machine learning classification models performed very well on the collected data, typically classifying data with accuracies of over 90%.

The paper is structured as follows: Section 2 presents the sensorised probe and its general characteristics, Section 3 outlines the data collection methodology, Section 4 presents the classification models used as well as their results, and lastly Section 5 presents a discussion of the results and future work.

2 A New Instrumented EIS Biopsy Needle

The sensorised EIS needle designs discussed earlier vary depending on their intended clinical use. In the same way, an EIS-capable needle designed specifically for prostate cancer biopsy must meet specific requirements. It is therefore essential to outline how a biopsy needle is used within the context of prostate biopsy, and how the probe would be implemented therein.

To implement such a device into a biopsy operation, slight adjustments to the conventional biopsy procedure are required. An ultrasound-guided prostate biopsy procedure begins with laying the patient down on their back, with their legs suspended in stirrups. The perineal tissue is numbed to reduce discomfort from inserting needles followed by the insertion of a US probe into the patient's rectum. The following steps are then performed:

- **Step 1**: A 16-gauge introducer needle with a cannula inserted coaxially through its shaft is inserted via the perineal muscles, as in Figure 2a, or rectal wall to the approximate area of the prostate under imaging guidance and placed within an intended target using real-time ultrasound images;
- **Step 2**: Once the introducer needle is positioned, the cannula is unscrewed from its base and removed from the needle's shaft while the introducer needle is kept in place, see Figure 2b;
- **Step 3**: A 18-gauge biopsy needle is then inserted coaxially through the introducer needle, see Figure 2c, wherein the area of the prostate can be sampled. The biopsy needle is connected to a spring-loaded mechanism. A finger-activated button deploys the inner stylet of the biopsy needle, where a sampling trough shears off and collected the target tissue for removal;
- **Step 4**: Once the sample is taken, the biopsy needle is removed from the introducer needle, and the biopsy sample extracted, as in Figure 2d, and the process may be repeated.

For a sensorised probe to be used in a clinical setting for biopsy, it must have minimal impact on the current, typical procedure. After consultation with urologists, it is suggested to incorporate the sensorized needle into the prostate biopsy procedure with an extra step introduced, to be performed between Step 2 and Step 3:

- **Step 2.5**: Following Step 2, and with the introducer needle positioned in the prostate, insert the sensorised needle probe, as in Figure 2e. The surgeon simultaneously uses the real-time image guidance and the EIS data that the sensorised needle probe reports to aid in localising the target lesion.

The core of the idea is that in Step 2.5 the operator maps out the boundaries of the lesion relative to the rest of the prostate, creating a zone in which the electrical impedance is known to be characteristic of malignancy or sufficiently different from that of benign tissue. Thereafter, the sensorised needle can be removed and steps 3 and 4 can be performed as in the original procedure. As a result, samples can then be taken with better knowledge of the location of the lesions relative to the needle tip.

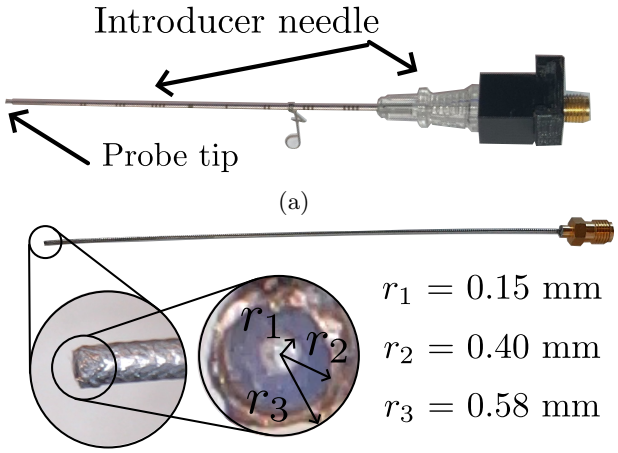

Fig. 3: a Sensorised electrode in introducer needle. b Sensorised electrode with macro shots of needle end and needle tip showing coaxial configuration.

The probe is composed of a coaxial cable electrode (Mouser, model 095-902-462-009) inserted in a rigid surgical introducer needle (Argon Medical Devices, model MCXS1815LX), as seen in Figure 3a. Seen in Figure 3b is the woven shielding of the coaxial cable, which acts as the outside electrode, and the inner concentric cable as the inner electrode. Both the outer and inner electrodes are made of stainless steel, which is bio-compatible, sterilisable, and rigid enough to avoid bending during steering in tissue. The coaxial cable's inner electrode has an outer diameter of 0.30 mm, while the outer electrode has an inner diameter of 0.80 mm and an outer diameter of 1.16 mm, see the right side of Figure 3b. The coaxial cable's outer diameter is small enough that it remains compatible with the 18 gauge biopsy needles that are often used in prostate biopsy.

The introducer needle is also constructed of extruded stainless steel. The electrodes have a separation distance of approximately 0.25 mm. In between the electrodes is an insulating Teflon sheath. The EIS probe requires a small 3D-printed part to rigidly couple with the introducer needle before connecting to the data transfer wires. With this implementation, and despite the additional step added, the inclusion of the EIS probe does not interfere with the other biopsy instrumentation and their operation.

3 Data collection

A dataset was collected for the purpose of validating the new sensorised biopsy needle. It consists of poultry pectoral muscle (PPM), poultry ventral muscle (PVM), bovine muscle (ML), porcine muscle (IM), bovine liver (BL), ovine muscle (OM), bovine kidney (KN), salmon tissue (ST), sole tissue (SoT), porcine cardiac tissue (PC), poultry cardiac tissue (PoC), and poultry liver (PL). All the *ex-vivo* tissue was purchased from a local grocer or butcher. To collect electrical impedance spectra, the needle probe is connected to a research impedance spectroscopy analyzer (Eliko, model Quadra impedance spectroscopy analyzer). The dataset measured 15 discrete frequencies across 1 to 349 kHz and between 200 and 250 measurements were taken for each tissue class.

Data collection was performed using the following protocol:

1. Samples being analyzed are placed in a refrigerator to reach the same temperature.
2. After 2 hours, samples are removed, and cut into either 4 or 5 separate 30×30 mm pieces.

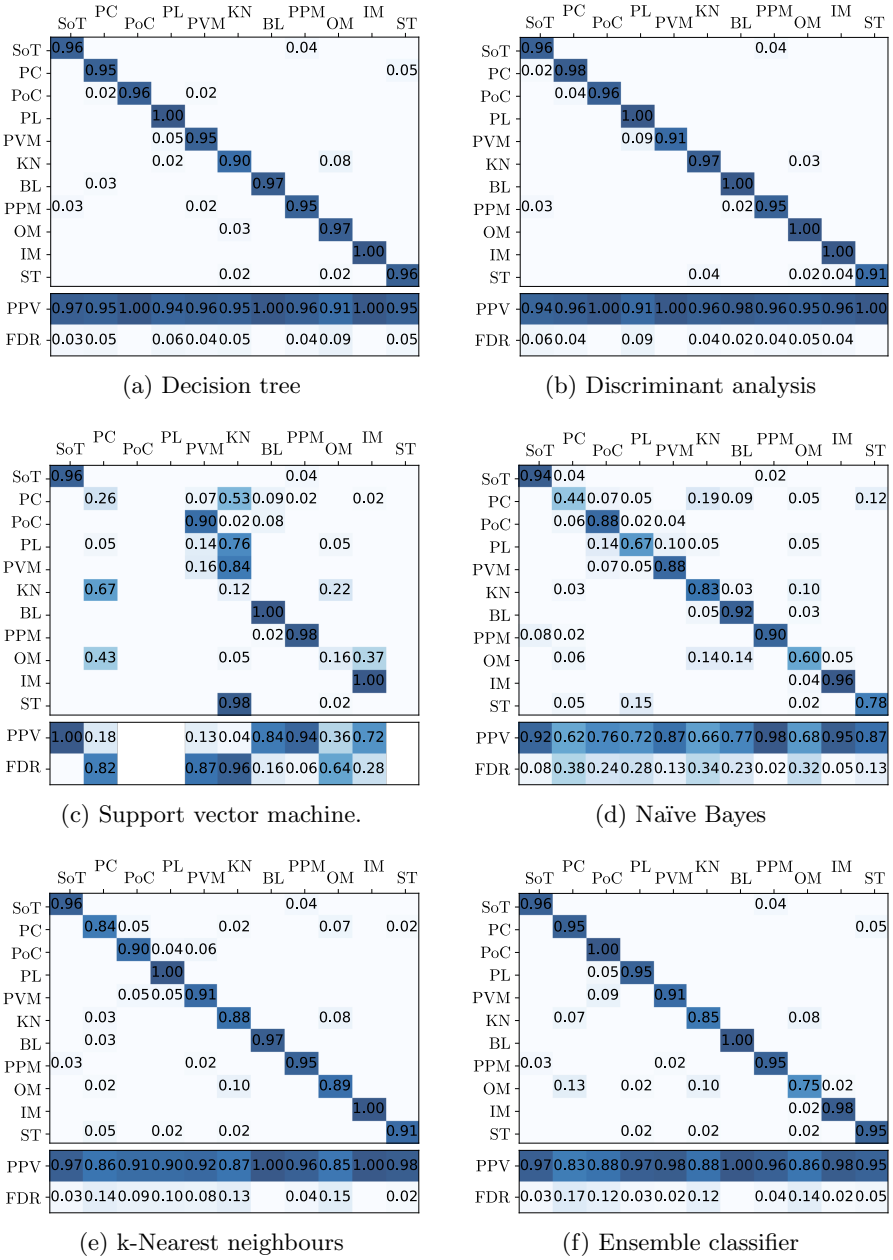

(a) Decision tree

(b) Discriminant analysis

(c) Support vector machine.

(d) Naïve Bayes

(e) k-Nearest neighbours

(f) Ensemble classifier

Fig. 4: Confusion matrices for a single instance of the classifiers trained and validated on collected EIS dataset.

3. Samples are placed on an insulating surface, in this case a board of high density polyethylene.
4. The needle probe is inserted into 5 different locations throughout the volume of the sample, and the EIS data is collected 10 times at each location.
5. Each location is measured continuously for 3-5 seconds at a measurement rate of 1000 Hz. The measurements are averaged to minimise noise during data collection.

4 EIS Tissue Classification

In order to validate the probe design presented and its measurements, the collected spectra from each tissue class will be classified via six different machine-learning classification algorithms. All classifiers used 10 k-folds cross-validation, non-normalised data, and were trained without performing any hyper-parameter optimisation. First, 2650 of the total 3650 spectra are pulled to use as the train and test sets. The training dataset consists of 2120 randomly selected entries from all classes with their corresponding labels, and the test set consists of the remaining 530 spectra. The classifiers are:

1. Decision tree (DT) algorithm with a maximum number of splits of 3199 and pruning;
2. Discriminant analysis (DA) algorithm with a linear discriminant kernel;
3. Naïve Bayes (NB) classifier using multi-variate Gaussian distributions;
4. K-nearest neighbour (kNN) using a single neighbour;
5. Support vector machine (SVM) with a polynomial of order 3; and
6. Ensemble classifier (EC) of multiple decision tree classifiers trained on overlapping sub-sets of the training dataset.

Each classifier was evaluated on four common metrics: accuracy, macro-precision (MP), macro-sensitivity (MS), and macro-f1 score (f1). The classification results are tabulated in Table 1 and the corresponding confusion matrices are shown in Figure 4.

Table 1: Classification metrics for collected data. All values are in %. Best individual metrics are bolded.

Classifier	Accuracy	MP	MS	f1
Decision tree	98.77	92.70	93.13	92.86
Discriminant analysis	**99.45**	**97.06**	**96.77**	**96.81**
Naïve Bayes	95.86	76.95	77.13	75.63
k-Nearest neighbours	98.73	92.74	93.39	92.90
Support vector machine	89.67	51.09	40.50	37.07
Ensemble classifier	98.80	93.64	93.59	93.52

The best overall performance is seen with the DA classifier providing an overall classification accuracy of 99.45%. The other classifiers performed similarly with classification accuracies greater than 90%, with the exception of NB, which performed slightly worse overall with an accuracy of 95.86%, and the SVM, with an accuracy of 89.67%. The DT, DA, kNN, and ensemble classifiers all showed sensitivity's, an important metric in clinical classification, greater than 90%.

5 Discussion and Conclusion

A new sensorised probe for use in identifying tissue at the tip of a biopsy introducer needle was presented in this publication. With it, a large *ex-vivo* dataset was collected. The data was used to train several down-stream

machine learning classification models, and did so with a high degree of accuracy. By using the performance of the classifiers as a proxy for the probes capability to take repeatable and accurate measurements of tissue, it can be inferred that the probe should be able to distinguish human prostate tissue. This device could be employed in a clinical setting to aid in the characterisation of healthy and malignant tissue to improve biopsy operations.

Still with these encouraging results, the spatial measurement properties of the probe have not yet been quantified. Work is presently underway to do so which will further demonstrate the probes ability to be employed in a clinical setting. Furthermore, *ex-vivo* human trials must be performed to confirm the suspicion that the probe can in fact distinguish human prostate tissue specifically.

References

1. Ahn, B.M., Kim, J., Ian, L., Rha, K.H., Kim, H.J.: Mechanical property characterization of prostate cancer using a minimally motorized indenter in an ex vivo indentation experiment. Urology **76**(4), 1007–1011 (2010)
2. Ahn, B., Lorenzo, E.I.S., Rha, K.H., Kim, H.J., Kim, J.: Robotic palpation-based mechanical property mapping for diagnosis of prostate cancer. Journal of endourology **25**(5), 851–857 (2011)
3. Aubertin, K., Trinh, V.Q., Jermyn, M., Baksic, P., Grosset, A.A., Desroches, J., St-Arnaud, K., Birlea, M., Vladoiu, M.C., Latour, M., et al.: Mesoscopic characterization of prostate cancer using raman spectroscopy: potential for diagnostics and therapeutics. BJU international **122**(2), 326–336 (2018)
4. Bell, N., Gorber, S.C., Shane, A., Joffres, M., Singh, H., Dickinson, J., Shaw, E., Dunfield, L., Tonelli, M., on Preventive Health Care, C.T.F., et al.: Recommendations on screening for prostate cancer with the prostate-specific antigen test. Cmaj **186**(16), 1225–1234 (2014)
5. Bidgoli, H.A., Schieda, N., Rossa, C.: On the sensitivity of bevelled and conical coaxial needle probes for dielectric spectroscopy. IEEE Transactions on Instrumentation and Measurement (2023)
6. Chhikara, B.S., Parang, K.: Global cancer statistics 2022: the trends projection analysis. Chemical Biology Letters **10**(1), 451–451 (2023)
7. de Gorski, A., Rouprêt, M., Peyronnet, B., Le Cossec, C., Granger, B., Comperat, E., Cussenot, O., Renard-Penna, R., Mozer, P.: Accuracy of magnetic resonance imaging/ultrasound fusion targeted biopsies to diagnose clinically significant prostate cancer in enlarged compared to smaller prostates. The Journal of urology **194**(3), 669–673 (2015)
8. Groskopf, J., Schalken, J., Rittenhouse, H.: Pca3. Prostate Cancer Screening pp. 233–241 (2009)
9. Grossi, M., Riccò, B.: Electrical impedance spectroscopy (eis) for biological analysis and food characterization: A review. Journal of sensors and sensor systems **6**(2), 303–325 (2017)
10. Halonen, S., Kari, J., Ahonen, P., Elomaa, T., Annus, P., Kronstrom, K.: Biopsy needle including bioimpedance probe with optimized sensitivity distribution. Int. J. Bioelectromagn. **17**(1), 26–30 (2015)
11. Halonen, S., Kari, J., Ahonen, P., Kronström, K., Hyttinen, J.: Real-time bioimpedance-based biopsy needle can identify tissue type with high spatial accuracy. Annals of biomedical engineering **47**(3), 836–851 (2019)
12. Halter, R.J., Hartov, A., Heaney, J.A., Paulsen, K.D., Schned, A.R.: Electrical impedance spectroscopy of the human prostate. IEEE Transactions on Biomedical Engineering **54**(7), 1321–1327 (2007)
13. Halter, R.J., Mishra, V., Bouayad, H., Manwaring, P., Heaney, J., Schned, A.: Electrical property-based biopsy for prostate cancer detection and assessment. In: Energy-based Treatment of Tissue and Assessment VI. vol. 7901, pp. 275–283. SPIE (2011)
14. Kachuri, L., De, P., Ellison, L., Semenciw, R.: Cancer incidence, mortality and survival trends in canada, 1970-2007. Chronic diseases and injuries in canada **33**(2) (2013)
15. Kaneko, M., Sugano, D., Lebastchi, A.H., Duddalwar, V., Nabhani, J., Haiman, C., Gill, I.S., Cacciamani, G.E., Abreu, A.L.: Techniques and outcomes of mri-trus fusion prostate biopsy. Current urology reports **22**, 1–12 (2021)
16. Kent, B., Rossa, C.: Electric impedance spectroscopy feature extraction for tissue classification with electrode embedded surgical needles through a modified forward stepwise method. Computers in Biology and Medicine **135**, 104522 (2021)
17. Kent, B., Rossa, C.: Development of a tissue discrimination electrode embedded surgical needle using vibro-tactile feedback derived from electric impedance spectroscopy. Medical & Biological Engineering & Computing pp. 1–13 (2022)

18. Lomas, D.J., Ahmed, H.U.: All change in the prostate cancer diagnostic pathway. Nature reviews Clinical oncology **17**(6), 372–381 (2020)
19. McDermott, C., Bidgoli, H.A., Rossa, C.: Observation of the ultrasonic vibration potential with an instrumented coaxial needle probe. In: 2023 IEEE International Instrumentation and Measurement Technology Conference (I2MTC). pp. 1–6. IEEE (2023)
20. McDermott, C., Lovett, S., Rossa, C.: Improved bioimpedance spectroscopy tissue classification through data augmentation from generative adversarial networks. Medical & Biological Engineering & Computing pp. 1–13 (2023)
21. Mishra, V., Bouayad, H., Schned, A., Hartov, A., Heaney, J., Halter, R.J.: A real-time electrical impedance sensing biopsy needle. IEEE transactions on biomedical engineering **59**(12), 3327–3336 (2012)
22. Mishra, V., Schned, A., Hartov, A., Heaney, J., Seigne, J., Halter, R.: Electrical property sensing biopsy needle for prostate cancer detection. The Prostate **73**(15), 1603–1613 (2013)
23. Nam, R.K., Klotz, L.H.: Trends in prostate cancer screening: Canada. Prostate Cancer Screening pp. 23–33 (2009)
24. Park, J., Jeong, Y., Kim, J., Gu, J., Wang, J., Park, I.: Biopsy needle integrated with multi-modal physical/-chemical sensor array. Biosensors and Bioelectronics **148**, 111822 (2020)
25. Verma, S., Choyke, P.L., Eberhardt, S.C., Oto, A., Tempany, C.M., Turkbey, B., Rosenkrantz, A.B.: The current state of mr imaging–targeted biopsy techniques for detection of prostate cancer. Radiology **285**(2), 343–356 (2017)
26. Vert, M., Doi, Y., Hellwich, K.H., Hess, M., Hodge, P., Kubisa, P., Rinaudo, M., Schué, F.: Terminology for biorelated polymers and applications (iupac recommendations 2012). Pure and Applied Chemistry **84**(2), 377–410 (2012)
27. Yun, J., Kang, G., Park, Y., Kim, H.W., Cha, J.J., Lee, J.H.: Electrochemical impedance spectroscopy with interdigitated electrodes at the end of hypodermic needle for depth profiling of biotissues. Sensors and Actuators B: Chemical **237**, 984–991 (2016)
28. Yun, J., Kim, H.W., Park, Y., Cha, J.J., Lee, J.Z., Shin, D.G., Lee, J.H.: Micro electrical impedance spectroscopy on a needle for ex vivo discrimination between human normal and cancer renal tissues. Biomicrofluidics **10**(3), 034109 (2016)